ISSN 1023-1935, Russian Journal of Electrochemistry, 2020, Vol. 56, No. 2, pp. 132–138. © Pleiades Publishing, Ltd., 2020.
Russian Text © The Author(s), 2020, published in Elektrokhimiya, 2020, Vol. 56, No. 2, pp. 141–148.

Three-Layered Membranes for Planar Solid Oxide Fuel Cells of the Electrolyte-Supported Design: Characteristics and Applications[1]

E. A. Agarkova[a, *], D. A. Agarkov[a, b], I. N. Burmistrov[a, b, **], O. Yu. Zadorozhnaya[c], D. V. Yalovenko[a], Yu. K. Nepochatov[c], and S. I. Bredikhin[a, b]

[a] *Institute of Solid State Physics, Russian Academy of Sciences, Chernogolovka, Moscow oblast, 142432 Russia*
[b] *Moscow Institute of Physics and Technology (State University), Dolgoprudnyi, Moscow oblast, 117303 Russia*
[c] *NEVZ-Ceramics, Novosibirsk, 630048 Russia*
**e-mail: stepanova.ea@issp.ac.ru*
***e-mail: buril@issp.ac.ru*

Received October 9, 2018; revised December 11, 2018; accepted July 4, 2019

Abstract—Three-layered ceramic membranes based on stabilized zirconia for planar solid-oxide fuel cell (SOFC) are prepared by the tape casting method. The external layers containing 94 mol % ZrO_2–6 mol % Sc_2O_3 provide the enhanced mechanical stability; the central layer has the composition of 89 mol % ZrO_2–10 mol % Sc_2O_3–1 mol % Y_2O_3 which has the highest anionic conductivity in the series of solid solutions ZrO_2–Y_2O_3–Sc_2O_3. Studying the mechanical characteristics shows that the ultimate strength (bending strength) of these membranes much exceeds the value typical of single-layered samples. The anionic conductivity of three-layered ceramics is studied by the impedance spectroscopy in the frequency range from 1Hz to 1 MHz. Membrane-electrode assemblies for SOFCs are fabricated and their electrochemical properties are studied under the conditions of fuel cell operation.

Keywords: multilayered membranes, anionic conductivity, solid electrolytes, three-point bending, voltammetric characteristic, impedance hodograph

DOI: 10.1134/S1023193520020020

INTRODUCTION

Solid oxide fuel cells (SOFCs) are among the most efficient and promising technologies of direct conversion of the chemical energy of hydrocarbon fuels to the electric (with 60% efficiency) and thermal energy (with the total efficiency above 90%) [1]. Electrolyte-supported planar fuel cells represent reliable high-technology versions of membrane-electrolyte assemblies (MEA) [2, 3]. This approach makes it possible to create automatic lines for carrying out all the operations of MEA production. The fuel cell obtained are characterized by stable parameters and mechanical stability [4]. The deposition methods used in their preparation are inexpensive and technological, which allows the final cost of electrochemical generators based on the SOFC technology to be substantially lowered.

The key component of a planar MEA for an electrolyte-supported SOFC is the anion-conducting membrane. First of all, it is this membrane that bears the main mechanical load and, secondly, its resistance is about a half of the total internal resistance of the fuel cell [5]. Thus, the optimal thickness of the supporting membrane is the result of competition of conflicting optimization principles: the decrease in the membrane thickness lowers down the losses caused by the ionic current, which has the positive effect on the total internal resistance of the fuel cell and the total efficiency of the electrochemical cell, whereas the increase in the thickness improves the mechanical characteristics and the total reliability of the system.

The mechanical properties of the anionic membrane can be improved by using multilayer structures [6] in which a part of layers are optimized not according to their electrochemical characteristics but according to their mechanical properties by refining their composition and microstructure. A series of our previous publications [7–9] was aimed at the development of highly efficient planar MEA for electrolyte-supported SOFCs [7–10]. In this paper we show the results of studying the electrochemical and mechani-

[1] Published on the basis of materials of the 5th All-Russia Conference "Fuel Cells and Power Plants Based on Them" (with international participation), Suzdal, 2018.

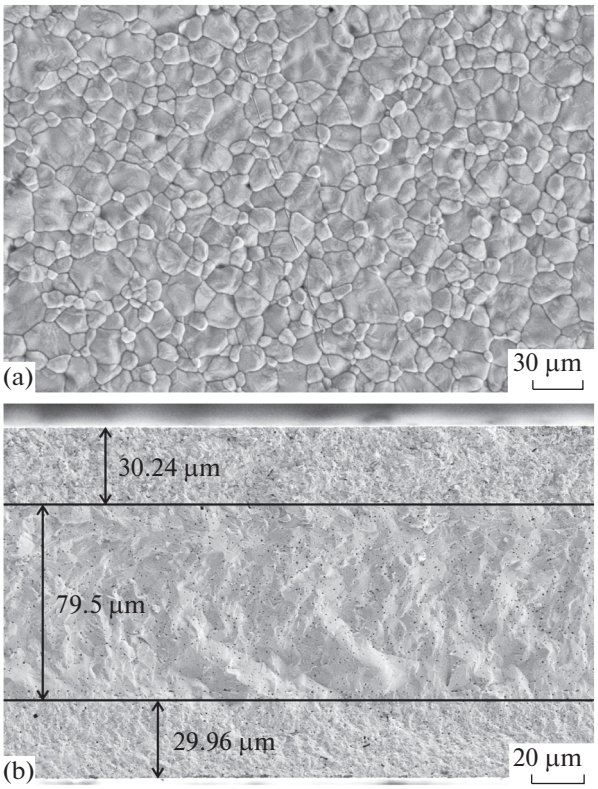

Fig. 1. SEM image of (a) the surface and (b) the cross-section of three-layered 6ScSZ/10Sc1YSZ/6ScSZ plates.

cal characteristics of three-layered solid-electrolyte membranes produced in Russia and also of membrane/electrode assemblies fabricated on their basis.

EXPRIMENTAL

As the precursors in the synthesis of membranes, we used powders of 6ScSZ ($(Sc_2O_3)_{0.06}$–$(ZrO_2)_{0.94}$) and 10Sc1YSZ ($(Sc_2O_3)_{0.1}$–$(Y_2O_3)_{0.01}$–$(ZrO_2)_{0.89}$) composites produced by Neokhim (Russia) [11]. The central layer was made of 10Sc1YSZ: in our previous studies of single-crystal samples, we have shown that zirconium dioxide doped with 10 mol % scandia and 1 mol % yttria or ceria demonstrates the maximum anionic conductivity [12–14]. The 6ScSZ composition demonstrated the high mechanical characteristics at the retention of sufficient anionic conductivity [15, 16]. The powders were produced by codeposition followed by annealing at different temperatures.

The anion-conducting membranes were made by casting on a moving tape, which was followed by vacuum delamination of sheets with different anion-conducting composition to obtain three-layered stacks. After this, the stacks were annealed at high temperature. Figure 1 shows microimages of their surface and cross-section obtained under a scanning electron microscope (SEM). The SEM studies were carried out

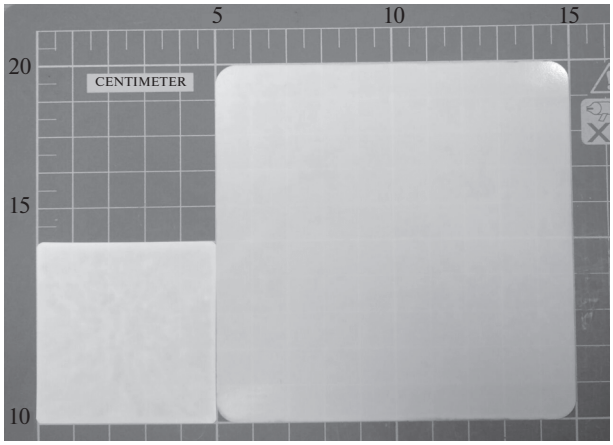

Fig. 2. Image of three-layered plates of the 6ScSZ/10Sc1YSZ/6ScSZ composite.

by means of Supra 50VP microscope (CarlZeiss, UK). As follows from Fig. 1a, the surface structure of the thus synthesized ceramics was dense, fine-grained, the grain size did not exceed 3 μm. The cleavage image (Fig. 1b) demonstrated the three-layered sandwich structure of 6ScSZ/10Sc1YSZ/6ScSZ with good adhesion of layers. The thickness of 6ScSZ and 10Sc1YSZ layers was 30 and 80 μm, respectively. The external layers demonstrated the high density of defects such as grain boundaries and packing defects, which prevented the development of microcracks at deformation of samples. The central layer was more uniform, the size of individual grains was above 5 μm, the grain boundaries were weakly distinguishable. Individual pores of less than 1 μm which formed no connected system and were unable to affect the gas permeability and transport characteristics of synthesized membranes were also present. The prepared membranes were shaped as squares with truncated corners and sides of 100 or 50 mm (Fig. 2).

The conduction and the mechanical properties of membranes were compared with analogous properties of anion-conducting membranes of the composition 10Sc1CeSZ ($(Sc_2O_3)_{0.1}$–$(CeO_2)_{0.01}$–$(ZrO_2)_{0.89}$) and the thickness of 150 μm produced by H.C. Starck (Germany) and also with the single-layered anion-conducting membrane of the composition 10Sc1YSZ and the thickness of 240 μm produced by NEVZ-Ceramics (Novosibirsk, Russia) [10].

The strength characteristics were assessed by the method of three-point bending on the setup Instron 1195. The samples of 24 × 9 mm were fixed by a facility made of single-crystal sapphire designed for three-point bending measurements; the distance between the extreme points at the bottom of the contact was 21 mm; the top loading point was at equal distances from the lower points (Fig. 3). The deformation of samples was carried out at a rate of 0.5 mm/min at

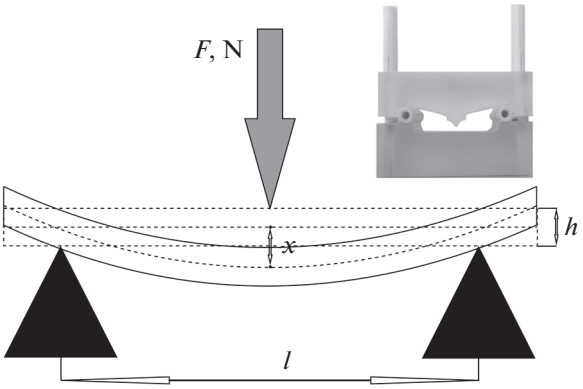

Fig. 3. Scheme and photograph of a sapphire setup for measuring the mechanical strength for bending of planar solid-electrolyte samples.

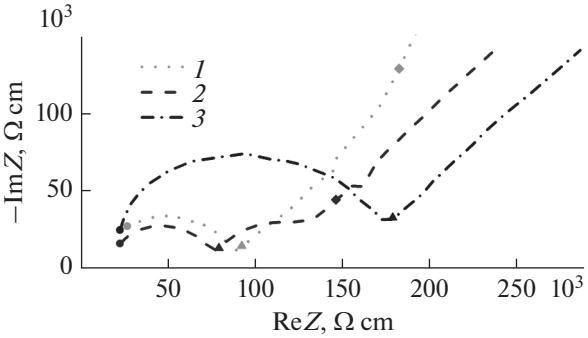

Fig. 4. Impedance hodographs of anionic membranes produced by (*1*) Stark, (*2* and *3*) NEVZ-Ceramics of the (*2*) single and (*3*) three-layered design measured in air at 350°C. Circles, triangles, and rhombs correspond to frequencies of 1 MHz, 10 kHz, and 100 Hz, respectively.

room temperature. The bending strength was calculated according to the formula

$$\sigma = \frac{3Fl}{2ah^2}, \quad (1)$$

where F is the ultimate mechanical load at which membrane's destruction takes place, l is the distance between the extreme points of the contact, a is the sample width, and h is its thickness.

To measure the transport properties by the two-contact 4-wire sensing method, the plane-parallel plates of 7 × 7 mm^2 were fabricated on which platinum electrodes were applied (platinum paste CL11-5100 produced by Heraeus, Germany), which was followed by annealing at temperature of 950°C for 10 min.

The temperature dependence of the anionic conductivity was studied by means of an impedance analyzer Solartron SI 1260 in the temperature range from 350 to 850°C in steps of 50°C. The frequency range of measurements was from 1 Hz to 1 MHz, the signal amplitude was 24 mV. Figure 4 exemplifies the impedance hodographs for anionic membranes of the single-layered [(*1*) H.C. Starck, (*3*) NEVZ-Ceramics] and three-layered [(*2*) NEVZ-Ceramics)] design obtained in air at 350°C. The spectra were analyzed by using the ZView software and the method of equivalent circuits.

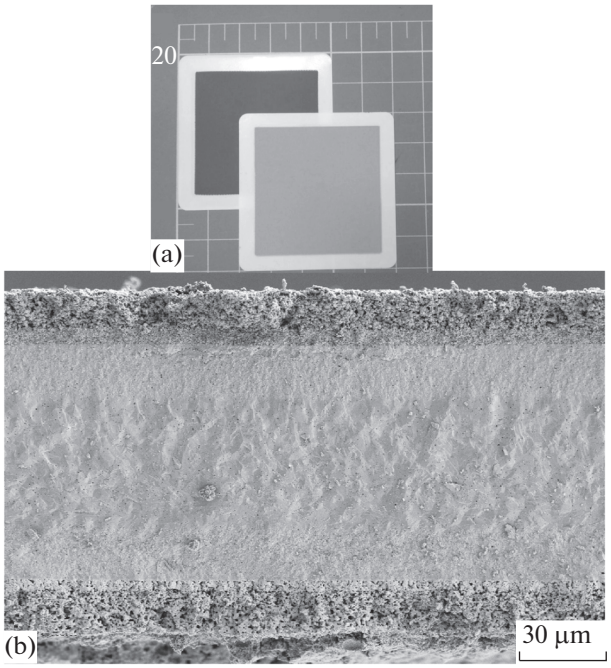

Fig. 5. (a) The structure of layers in multilayered ceramic membrane-electrode assemblies and (b) the SEM image of their cross-section.

Using three-layered plates of 50 × 50 mm^2, the membrane-electrode assemblies were prepared with multilayered electrodes based on the following powders: GDC ($Ce_{0.9}Gd_{0.1}O_{2-\delta}$, FuelCellMaterials, USA) and LSM [$(La_{0.8}Sr_{0.2})_{0.95}MnO_{3-\delta}$, Institute of Solid State Physics, RAS, Russia] for the cathode and also GDC, NiO (Aldrich, USA) and 10Sc1CeSZ (89 mol % ZrO_2 + 10 mol % Sc_2O_3 + 1 mol % CeO_2, Qingdao Terio, China) for the anode. These precursors were subjected to preliminary thermal treatment [17] and then used in the preparation of composite powders by milling in a planetary mill. The cathode and the anode were applied by screen printing. After their application, the fuel cells were co-sintered at 1350°C. The surface of thus prepared electrodes was 16 cm^2 (square of 40 × 40 mm^2). Figure 5 shows SEM images of the electrode surface and cross section.

The electrochemical characteristics of fuel cell prototypes were studied on a gas-temperature bench at the working temperature of 850°C, the oxidizer and the fuel represented the mixtures O_2/N_2 = 21/79 and H_2/N_2 = 50/50, respectively. Voltammetric characteristics and hodographs of impedance spectra were obtained by means of a potentiostat-galvanostat and impedance meter Reference 3000 with an attachment

Reference 30K Booster (Gamry, Italy). The impedance spectra were measured in the frequency range of 0.1 Hz–300 kHz at the constant current load of 0.44 A/cm^2, the ac signal amplitude was 20 mV.

RESULTS AND DISCUSSSION

Mechanical Characteristics

In the previous studies [7] we have shown that when the thickness of the supporting membrane is decreased down to 250 μm, the further operations on the preparation of the electrode system are severely complicated by the increased brittleness of the solid-electrolyte plate. To improve the mechanical characteristics of electrolyte membranes, it was proposed to use a three-layered structure in which the central layer which offers the minimum resistance to the transport of oxygen anions was prepared from completely stabilized zirconia of the following composition: $(Sc_2O_3)_{0.1}$–$(Y_2O_3)_{0.01}$–$(ZrO_2)_{0.89}$. To prepare the outer layers, we used the tetragonal $(Sc_2O_3)_{0.06}$–$(ZrO_2)_{0.94}$ composition with the high density of extensive defects in sintered ceramics [18], which efficiently prevented the propagation of microcracks and improved the mechanical characteristics of the three-layered stack.

Figure 6 exemplifies the load curves obtained by the method of three-point bending. The tests were carried out with 6 samples of each type after which the results were averaged. Table 1 shows the results of mechanical tests averaged over the series of measurements.

According to Fig. 6 and Table 1, the three-layered membranes demonstrated the better characteristics as regards cross-bending characteristics (up to 1.4 mm against 0.5 and 1 mm for single-layered membranes). In average, the ultimate bending strength of a three-layered membrane was 560 MPa (for single-layered membranes, this value was 273 and 286 MPa).

When the membranes used in samples were subjected to strength tests, they demonstrated considerable deflection (up to 1.4 mm) which made impossible to find the Young modulus values. To assess the elastic modulus, we used the ratio of the ultimate strength to the maximum bending at which the destruction of sample occurred. The ratios found for three-layered membranes produced by NEVZ-Ceramics and H.C. Stark companies were 445 and 413 MPa/mm, i.e., almost a half of this value of the single-layered membrane (NEVZ-Ceramics). Thus, by decreasing the supporting-electrolyte thickness and, hence, its elastic modulus, we can allow a substantial deformation of these membranes without generating any critical stresses in the supporting membrane. On the other hand, the use of the three-layered structure substantially improves the strength characteristics of this issue.

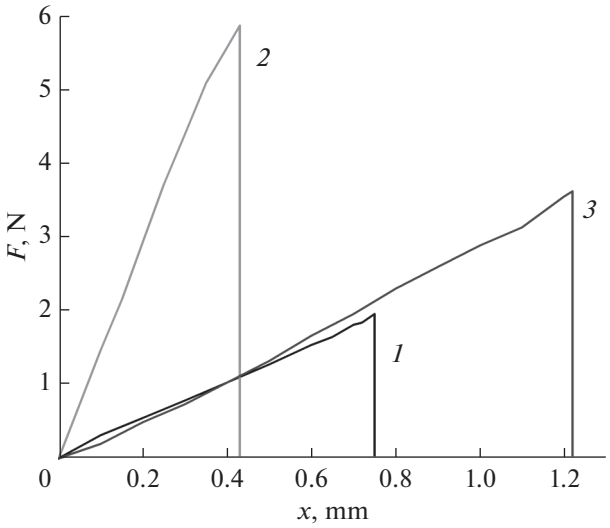

Fig. 6. Load curves obtained by the method of three-point bending at room temperature for (*1*) membrane produced by H.C. Starck and (*2* and *3*) single and three-layered membranes produced by NEVZ-Ceramics, respectively.

Transport Characteristics

Figure 7 shows the temperature dependence of the total (ignoring the single- or three-layered structure) ionic conductivity of membranes under study. For a comparison, Fig. 7 shows also the data for single crystals 6ScSZ and 10Sc1YSZ [12, 19]. The conductivity of single-layered membranes is close to that of the

Table 1. Results of measurements of mechanical characteristics of anion-conducting membranes

Membranes	1	2	3
	H.C. Starck	NEVZ-Ceramics, single-layered sample	NEVZ-Ceramics, three-layered sample
Thickness, μm	150	240	140
Average maximum bending x, mm	0.66 ± 0.06	0.37 ± 0.02	1.255 ± 0.04
Average ultimate strength σ, MPa	273 ± 25	286 ± 17	560 ± 25
Average ratio of ultimate strength to maximum bending σ/x, MPa/mm	413 ± 10	774 ± 30	445 ± 6

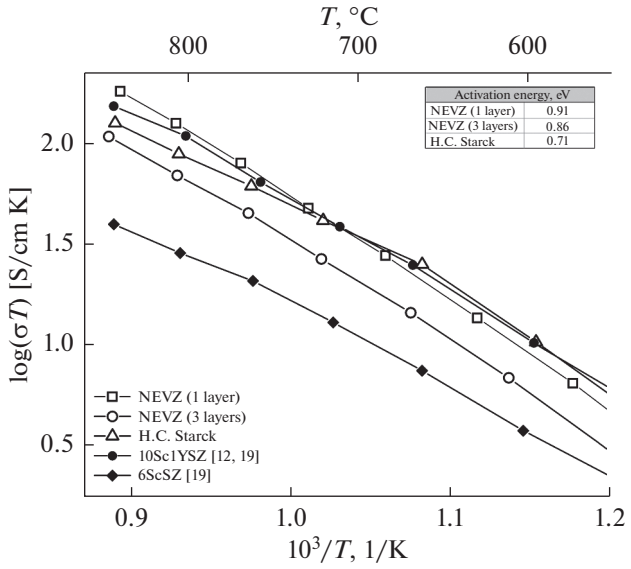

Fig. 7. Temperature dependence of the specific conductivity of membranes as compared with single crystals 6ScSZ and 10Sc1YSZ [12, 19].

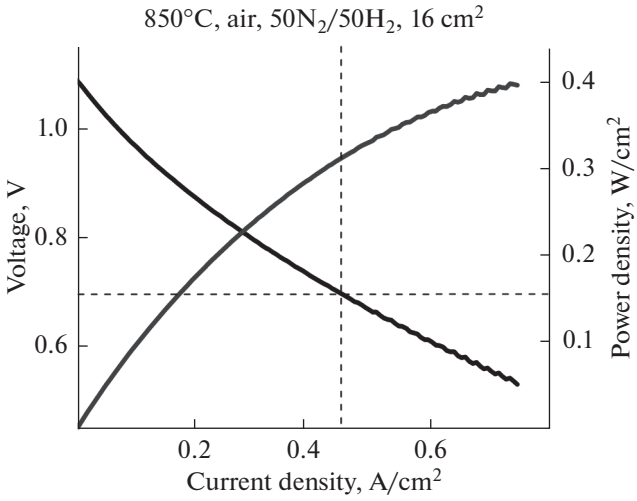

Fig. 8. Voltammetric and power characteristics of the membrane-electrode assembly based on three-layered membrane.

10Sc1YSZ single crystal, which suggests the insignificant effect of microstructure factors on the transport characteristics of electrolytes under study. In its turn, the conductivity of the three-layered membrane lies between its values for single crystals 6ScSZ and 10Sc1YSZ throughout the temperature region, which points to both the good adhesion of layers and the absence of additional weakly conducting phases in the region of contact between layers in the ceramic stack.

Table 2 shows the specific conductivity of ceramic and single-crystal samples at 850°C and also the activation energies in the temperature interval 600–850°C. In the whole temperature interval, the ionic conductivity of a three-layered membrane was somewhat lower than its values for single-layered membranes and reached 0.095 S/cm at 850°C, which, however, substantially exceeded the conductivity of 6ScSZ single crystal (0.036 S/cm). Thus, the use of the three-layered structure involving 6ScSZ as one of its components with the relatively low conductivity lowered down the total ionic conductivity of the stack by no more than 30% (850°C) as compared with the conductivity of the 10Sc1YSZ single crystal.

Table 2. Specific conductivity at 850°C and activation energy in the high-temperature region (600–850°C) for planar ceramic membranes and single crystals 6ScSZ and 10Sc1YSZ [12, 19]

Membrane or single crystal	Specific conductivity at 850°C, S/cm	Activation energy for $T = 600$–850°C, eV
NEVZ-Ceramics (1 layer)	0.160	0.91
NEVZ-Ceramics (3 layers)	0.095	0.86
H.C. Starck	0.111	0.71
10Sc1YSZ [12, 19]	0.134	0.81
6ScSZ [19]	0.036	0.67

Membrane-Electrode Assemblies

Figure 8 shows the voltammogram and the power characteristics of a MEA, which were measured with the use of artificial air as the oxidizer and the hydrogen-nitrogen mixture $H_2/N_2 = 50/50$ as the fuel at 850°C. The open circuit potential was about 1.1 V, which pointed to gas-tightness and the absence of electronic conduction of the membrane. The power density at the working potential of 0.7 V exceeded 300 mW/cm^2, which confirmed the sufficiently low internal resistance of the MEA.

To determine the structure of the internal resistance of thus prepared MEA, we measured its impedance spectra. Figure 9 shows a hodograph of impedance spectra for a MEA of SOFC, measured at the constant current load $I_{load} = 0.44$ A/cm^2. The analysis of impedance spectrum showed that under these experimental conditions, the total internal resistance was about 0.62 Ω/cm^2, and the ohmic losses were 0.28 Ω/cm^2, which amounts to ca. 45% of the total resistance of MEA. It deserves mention that the expected value of the resistance of the anionic membrane determined from the temperature dependence of ionic conductivity (Fig. 6) was 0.16 Ω/cm^2 (26% of the internal resistance of the SOFC), which pointed to the additional ohmic losses associated with the presence of layered-structure-induced resistance and/or

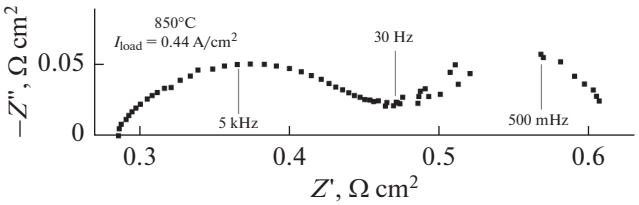

Fig. 9. Hodograph of impedance spectrum for membrane-electrode assembly based on three-layered membrane.

the specific morphology features of the internal interfaces in MEA.

Thus, based on electrochemical characteristics found here, we can conclude that the three-layered solid-electrolyte membranes we prepared to be used as the support in planar electrolyte-supported SOFCs. To increase further the efficiency of electrolyte-supported fuel cells, it is necessary to improve both the catalytic and transport characteristics of electrodes for SOFC MEAs.

CONCLUSIONS

It is shown that the use of relatively low-conducting components (6ScSZ) for the three-layered membrane structure on the basis of zirconia leads to the expected decrease in the ionic conduction; however, this decrease does not exceed 30% when compared with the standard samples of single-crystal 10Sc1YSZ. The electrochemical tests of MEAs with three-layered membranes demonstrated their sufficiently high power density equal to 300 mW/cm^2 at the cell voltage of 0.7 V and air used as the oxidant. The analysis of impedance spectra of MEAs demonstrated that the ohmic contribution into the total internal resistance of samples did not exceed 45%.

FUNDING

This study was supported by the Russian Scientific Foundation, grant no. 17-79-30071 "The development of scientifically substantiated ways to optimizing power and mass-dimensional characteristics of SOFC batteries of the planar design and the development of fuel processors for high-efficient transport and stationary power stations". The procedure of studying the temperature dependence of the anionic conductivity of membranes was developed within the frames of the State Project for the Institute of Solid-State Physics of the Russian Academy of Sciences.

CONFLICT OF INTERESTS

The authors declare the absence of any conflict of interests.

REFERENCES

1. Choudhury, A., Chandra, H., and Arora, A., Application of solid oxide fuel cell technology for power generation—A review, *Renewable Sustainable Energy Rev.*, 2013, vol. 20, p. 430.
2. Stelter, M., Reinert, A., Mai, B.E., and Kuznecov, M., Engineering aspects and hardware verificat solid oxide fuel cell stack design, *J. Power Sources*, 2006, vol. 154, p. 448.
3. Menzler, N.H., Malzbender, J., Schoderböck, P., Kauert, R., and Buchkremer, H.P., Sequential tape casting of anode-supported solid oxide fuel cells, *Fuel Cells*, 2014, vol. 14, p. 96.
4. Fleischhauer, F., Bermejo, R., Danzer, R., Mai, A., Graule, T., and Kuebler, J., Strength of an electrolyte supported solid oxide fuel cell, *J. Power Sources*, 2015, vol. 297, p. 158.
5. Hsieh, Y.D., Chan, Y.H., and Shy, S.S., Effects of pressurization and temperature on power generating characteristics and impedances of anode-supported and electrolyte-supported planar solid oxide fuel cells, *J. Power Sources*, 2015, vol. 299, p. 1.
6. Haydn, M., Ruettinger, M., Franco, T., Uhlenbruck, S., Jung, T., and Ortner, K., US Patent, 20160118680 A1, 2015.
7. Burmistrov, I., Agarkov, D., Bredikhin, S., Nepochatov, Y., Tiunova, O., and Zadorozhnaya, O., Multilayered electrolyte-supported SOFC based on NEVZ-Ceramics membranes, *ECS Trans.*, 2013, vol. 57, no. 1, p. 917.
8. Burmistrov, I.N., Agarkov, D.A., Tsybrov, F.M., and Bredikhin, S.I., Preparation of membrane-electrode assemblies of solid oxide fuel cells by co-sintering of electrodes, *Russ. J. Electrochem.*, 2016, vol. 52, p. 669.
9. Burmistrov, I.N., Agarkov, D.A., Korovkin, E.V., Yalovenko, D.V., and Bredikhin, S.I., Fabrication of membrane-electrode assemblies for solid oxide fuel cells by joint sintering of electrodes at high temperature, *Russ. J. Electrochem.*, 2017, vol. 53, p. 873.
10. Tiunova, O.V., Zadorozhnaya, O.Yu., Nepochatov, Yu.K., Burmistrov, I.N., Kuritsyna, I.E., and Bredikhin, S.I., Ceramic membranes based on scandium-stabilized ZrO_2 obtained by tape casting technique, *Russ. J. Electrochem.*, 2014, vol. 50, p. 719.
11. Sokolov, P.S., Karpyuk, P.V., Dosovitskiy, G.A., Volkov, P.A., Lyskov, N.V., Slyusar, I.V., and Dosovitskiy, A.E., Stabilized zirconia-based nanostructured powders for solid-oxide fuel cells, *Russ. J. Eletrochem.*, 2018, vol. 54, p. 464.
12. Kuritsyna, I.E., Bredikhin, S.I., Agarkov, D.A., Borik, M.A., Kulebyakin, A.V., Milovich, F.O., Lomonova, E.E., Myzina, V.A., and Tabachkova, N.Yu., Electrotransport characteristics of ceramic and single crystal materials with the $(ZrO_2)_{0.89}(Sc_2O_3)_{0.10}(Y_2O_3)_{0.01}$ composition, *Russ. J. Electrochem.*, 2018, vol. 54, p. 481.
13. Agarkov, D.A., Borik, M.A., Bredikhin, S.I., Kulebyakin, A.V., Kuritsyna, I.E., Lomonova, E.E., Milovich, F.O., Myzina, V.A., Osiko, V.V., Agarkova, E.A., and Tabachkova, N.Yu., Structure and transport properties of zirconia-based solid solution crystals co-doped with scandium and cerium oxides, *Russ. J. Electrochem.*, 2018, vol. 54, p. 459.

14. Agarkov, D.A., Borik, M.A., Bublik, V.T., Bredikhin, S.I., Chislov, A.S., Kulebyakin, A.V., Kuritsyna, I.E., Lomonova, E.E., Milovich, F.O., Myzina, V.A., Osiko, V.V., and Tabachkova, N.Yu., Structure and transport properties of melt grown Sc_2O_3 and CeO_2 doped ZrO_2 crystals, *Solid State Ionics*, 2018, vol. 322, p. 24.

15. Fleischhauer, F., Bermejo, R., Danzer, R., Mai, A., Graule, T., and Kuebler, J., High temperature mechanical properties of zirconia tapes used for electrolyte supported solid oxide fuel cells, *J. Power Sources*, 2015, vol. 273, p. 237.

16. Varanasi, C., Juneja, C., Chen, C., and Kumar, B., Electrical conductivity enhancement in heterogeneously doped scandia-stabilized zirconia, *J. Power Sources*, 2005, vol. 147(1–2), p. 128.

17. Burmistrov, I., Agarkov, D., Tartakovskii, I., Kharton, V., and Bredikhin, S., Performance optimization of cermet SOFC anodes: an evaluation of nanostructured Ni, *ECS Trans.*, 2015, vol. 68, no. 1, p. 1265.

18. Agarkov, D.A., Bredikhin, S.I., Burmistrov, I.N., Kuritsyna, I.E., Nepochatov, Yu.K., and Tiunova, O.V., Russian Patent 161024, 2016.

19. Borik, M.A., Bredikhin, S.I., Bublik, V.T., Kulebyakin, A.V., Kuritsyna, I.E., Lomonova, E.E., Milovich, F.O., Myzina, V.A., Osiko, V.V., Ryabochkina, P.A., and Tabachkova, N.Yu., Structure and conductivity of yttria and scandia doped zirconia crysrals grown by skull melting, *J. Am. Ceram. Soc.*, 2017, vol. 100(12), p. 5536.

Translated by T. Safonova

SPELL: 1. ok